Study on Surface Electricity. (XXI)*

On the Structure of Interfacial Double Layer Considered from the Behaviour of its Capacitance

Akira WATANABE, Fukuju TSUJI, Tokuro YASUDA and Shizuo UEDA**

(Tachi Laboratory)

Received February 22, 1956

The differential double layer capacities at mercury-0.1 N salt solution interfaces are measured by resonance method using dropping mercury electrodes, and the results are discussed from the viewpoint of double layer structure.

The capacity behaviours in this case have the same features as in the case of 1 N solutions, although they are reduced in magnitudes in all range of polarization. Tendencies of capacity minima near electrocapillary maximum potentials begin to appear in this case. These two results are quite in accord with the theory of double layer structure, because the diffuse double layer capacity, which is in series to the non-diffuse double layer capacity, has the very property and begins to predominate the whole capacity value as the solution becomes more dilute.

The humps near electrocapillary maxima become less evident, when the solutions are more dilute, which suggests that these phenomena of capacity humps are attributed to the property in the non-diffuse double layer. Contrary to apparent presumption, the capacity values at humps increase with anionic radii of salts in solutions. These are ascribed to the ionic polarizability at interfaces.

We have so far measured the differential double layer capacities at various mercury-salt solution interfaces by our resonance method, and many interesting features of their behaviours have been identified. In the foregoing papers were described details of the experimental devices[1] and the results of measurements with various 1 N salt solutions as the liquid phases of interfaces[2]. In view of the ultimate aim of the present authors, however, extension of our measuring method to more dilute salt solutions is indispensable for clarifying the structure of double layer. With this improvement the behaviours of the differential double layer capacities of mercury-0.1 N salt solution interfaces were determined and their behaviours were discussed from the viewpoint of double layer structure in connection with those at 1 N salt solutions.

---

* Read before the Semi-annual Meeting of this Institute, held June 11, 1955.

** 渡辺 昌, 辻 福寿, 安田 徳郎, 上田 静男

1. EXPERIMENTAL

As the concentration of the solution phase of the interface becomes less, the resistivity of the circuit becomes greater and its Q-value[3] smaller. Although the resistance of solution was taken into account in the preceding measurements by using substitution method, we shall discuss here the influence of the resistivity on the resonance phenomenon in detail.

(i) Resonance phenomenon of the circuit including resistivity

The principal resonance circuit used in our measurements is shown in Fig. 1,

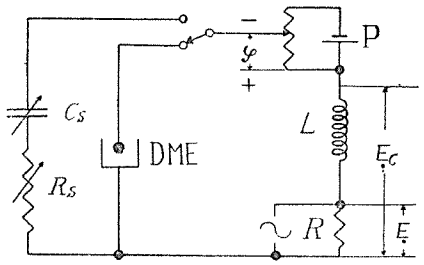

Fig. 1. Resonance circuit.

where DME is the dropping mercury electrode, P a potentiometer by which the bias voltage $-\varphi$ is applied to the mercury cathode, L the load inductance, R a small resistance to which an alternating voltage $\dot{E}$ is fed from a CR-valve oscillator and R_s and C_s are standard resistance and capacitance boxes used to calibrate the resistance and capacitance values of DME by substitution method.

The Q-value of this circuit, defined as the ratio of the resonance voltage $\dot{E}_c$ and input voltage $\dot{E}$, is given by

$$\dot{Q}=\frac{\dot{E}_c}{\dot{E}}=\frac{j(-1/\omega C)+R_0}{j(-1/\omega C)+(R_t+j\omega L)}=\frac{\dot{L}x+\dot{M}}{\dot{P}x+\dot{S}} \qquad (1)^*$$

where

$$\dot{L}=j, \quad \dot{M}=R_0, \quad \dot{P}=j,$$
$$\dot{S}=R_t+j\omega L \quad \text{and} \quad x=-1/\omega C. \qquad (2)$$

Here the small inner resistance of potentiometer is neglected. Because the interfacial capacitance becomes larger with the growth of mercury drop, we can consider x the variable of this equation. Now, when we put

$$a=\frac{\widehat{L\cdot M}}{L^2}-\frac{\widehat{P\cdot S}}{P}, \qquad \kappa=\frac{1}{2a}\left(\frac{M^2}{L^2}-\frac{S^2}{P^2}\right),$$

* C and R_0 are double layer capacitance and solution resistance, respectively.[1] $R_t=R+R_0$

$$b=\frac{\widehat{P\cdot S}}{P^2}-\kappa\,,\qquad c=\kappa^2-2\frac{\widehat{P\cdot S}}{P^2}\kappa+\frac{S^2}{P^2}\,, \tag{3}*$$

we can obtain the condition of maximum Q-value as follows:
In case $a<0$,
when

$$x=-\sqrt{c}-\kappa, \tag{4}$$

$$Q_{max}=\frac{L}{P}\sqrt{1-\frac{-a}{\sqrt{c}-b}}\,. \tag{5}$$

The calculation is simple, giving:
When

$$\frac{1}{\omega C}=\frac{\omega L}{2}\left(1+\sqrt{1+\frac{4R_t^2}{\omega^2L^2}}\right), \tag{6}$$

$$Q_{max}=\frac{\omega L}{2R_t}\left(1+\sqrt{1+\frac{4R_t^2}{\omega^2L^2}}\right). \tag{7}$$

These two equations give the resonance conditions of our experimental circuit, which tend to the ordinary resonance conditions as the total resistance R_t becomes zero.

(ii) Experimental method

The method of experiments is the same in principle as that in the foregoing papers,[1,2] except that the measuring frequencies are chosen which are far lower, i. e. from 15 to 60 cps, and that the frequency is changed to obtain its value which satisfies the resonance conditions at the last moment of the drop growth, contrary to the foregoing experiments where the load inductance was changed.

(iii) Results

The differential capacity values of double layer at mercury-0.1 N salt solution interfaces, obtained in this experiment, are summarized in Table 1. For brevity, detailed experimental conditions are not shown, the outlines of which are as follows:

$\varphi=0\sim-2.0$ V, $W=2.5\sim4.8$ mg,
$A=0.016\sim0.025$ cm^2, $T=2\sim4.5$ sec,
$f=15\sim60$ cps, $E=7.4$ mV (AC),
$L=4$ h (200 Ω) or 2 h (110 Ω),
$C=2.11\sim0.25$ μF.

2. DISCUSSION

The capacity behaviours in the case of 0.1 N solutions have the same features as in the case of 1 N solutions, as were given in the preceding paper in detail.[2] Here,

* The letters without dots show the moduli of each complex quantities, and the symbol $\widehat{\ }$ shows the scalar product of the two complex quantities.

Table 1. Differential double layer capacities at mercury-0.1N salt solutions.

$\mu F/cm^2$

Salts / φ(V)	KI	KBr	KCl	KF	KIO_3	$NaIO_3$	$KBrO_3$	$NaBrO_3$	$KClO_3$	KNO_3
0				33.34			47.27	56.44	43.58	28.16
-0.1			51.07	30.65			35.38	41.68	29.89	22.60
-0.2		61.87	34.61	28.74		67.13	30.45	31.70	25.60	19.10
-0.3	71.44	46.40	34.36	25.33	51.22	45.54	26.32	29.08	22.49	19.62
-0.4	60.89	45.05	35.83	22.27	39.22	37.38	26.92	28.39	22.56	21.28
-0.5	39.20	35.16	33.11	20.56	33.52	35.19	26.52	27.56	22.97	23.94
-0.6	23.59	24.02	25.41	18.99	27.63	28.59	24.65	26.06	24.41	25.90
-0.7	16.56	18.11	19.86	17.90	22.92	23.15	24.20	23.43	24.25	24.97
-0.8	14.56	15.61	18.39	17.57	20.50	20.09	20.96	20.13	23.00	21.21
-0.9	14.30	14.51	16.38	16.85	19.68	17.72	18.21	17.86	19.69	18.30
-1.0	14.68	13.87	15.84	15.61	17.30	16.71	16.29	16.81	17.33	17.58
-1.1	15.21	14.16	15.57	14.52	15.90	15.59	15.15	15.69	15.76	14.82
-1.2	15.99	14.45	14.52	14.72	14.88	14.72	14.51	14.02	14.22	14.20
-1.3	17.00	14.59	14.88	14.06	14.06		14.00	14.35	14.15	13.96
-1.4	17.87	16.08	14.35	14.50			13.29	14.74	13.66	13.48
-1.5	18.94	16.25	14.73	14.88			13.53	14.19	14.24	14.15
-1.6	22.63	16.85	15.84	15.36			14.25	14.19	14.55	14.17
-1.7		18.42	16.45	15.42			14.60	15.43	15.27	14.79
-1.8		19.95	17.63	16.59				16.70	15.85	15.21
-1.9			19.03	17.53					15.92	15.77
-2.0			20.60	19.49					17.89	15.93
φ_{max}(V)	0.440	0.410	0.581	0.610	0.860	0.895	0.720	0.740	0.760	0.700
t°C	21	21	22	22	22	22	22	24	22	22

C_0-$\boldsymbol{E}$ curves are shown of halide (Fig. 2) and oxy-anion (Fig. 3) solutions, separately. We shall discuss here also the results by dividing the polarization of mercury electrode in three regions, i. e. anodic ($\boldsymbol{E}>\boldsymbol{E}_a$), cathodic ($\boldsymbol{E}<0$) and zero regions ($\boldsymbol{E}\fallingdotseq 0$).[2]

(i) Anodic region

The order of the strength of anionic adsorption in this region is shown to be the same as the strength of the bonds between mercury and corresponding anion in this

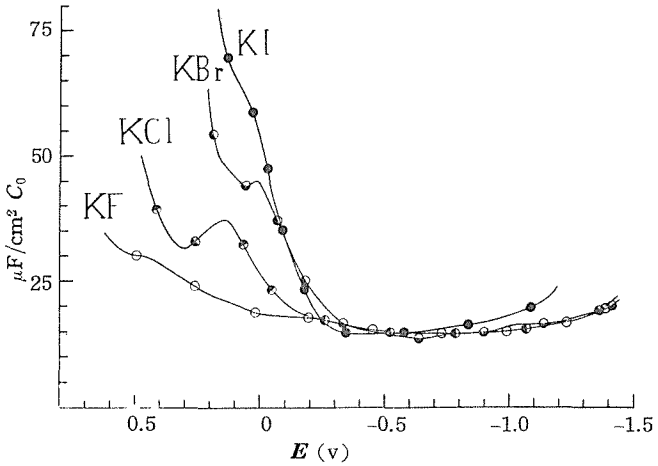

Fig. 2. 0.1N K-halides.

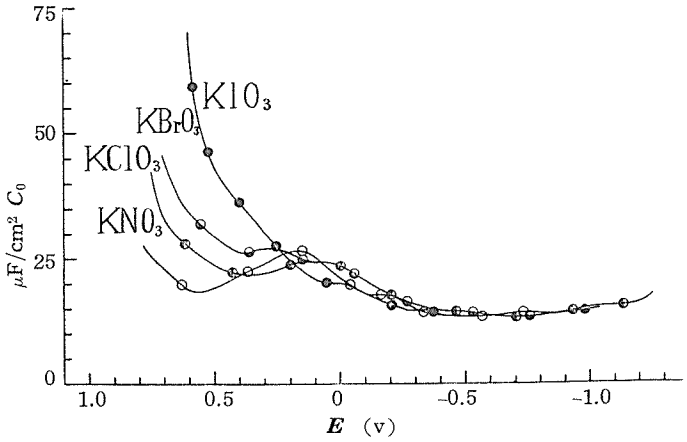

Fig. 3. 0.1N K-halogenates and -nitrate.

case also. This is evident from Figs. 2 and 3, where, for the sake of simplicity, halide and halogenate anions are compared separately. The solubilities of mercurous salts of halogenate are known to be in the order of, $IO_3' > BrO_3' > ClO_3'$.

(ii) Cathodic region

The capacity values in this region have flat minima of about 14~15 $\mu F/cm^2$. This is the same in character as in the case of 1 N solutions, but a little smaller in magnitude than in the latter case, which shall be explained later, where the structure of double layer is discussed.

(iii) Zero region

The characteristic feature in this region is the well-defined hump in capacity-bias voltage curve, although, in the case of iodide and fluoride, it is more or less masked and becomes less well-defined in the more dilute solutions, as is shown in Fig. 4.

This phenomenon of hump was shown in the preceding paper[2] to be intimately connected with the dielectric properties of the corresponding anion, because the capacity values at humps C_h are arranged in the order of anionic species, which is the same as the deformabilities of the respective anions.

Now, we shall discuss them by applying Grahame's model of the double layer structure[4] and making use of the equations derived by Devanathan[5].

The locus of specifically adsorbed (dehydrated) anions is called here "H-plane" and that of the hydrated adsorbed cations (or anions) "G-plane", outward of which stretches the Gouy diffuse double layer. The geometrical surface of mercury is called "M-plane", and the space between M- and H-planes constitutes the so-called non-diffuse layer (Fig. 5). Fig. 6 shows the schematic potential behaviour in the interfacial double layer, where ϕ's are the Grahame's "cavity potential" of the individual planes with reference to that of the bulk of solution phase. We shall designate the integral

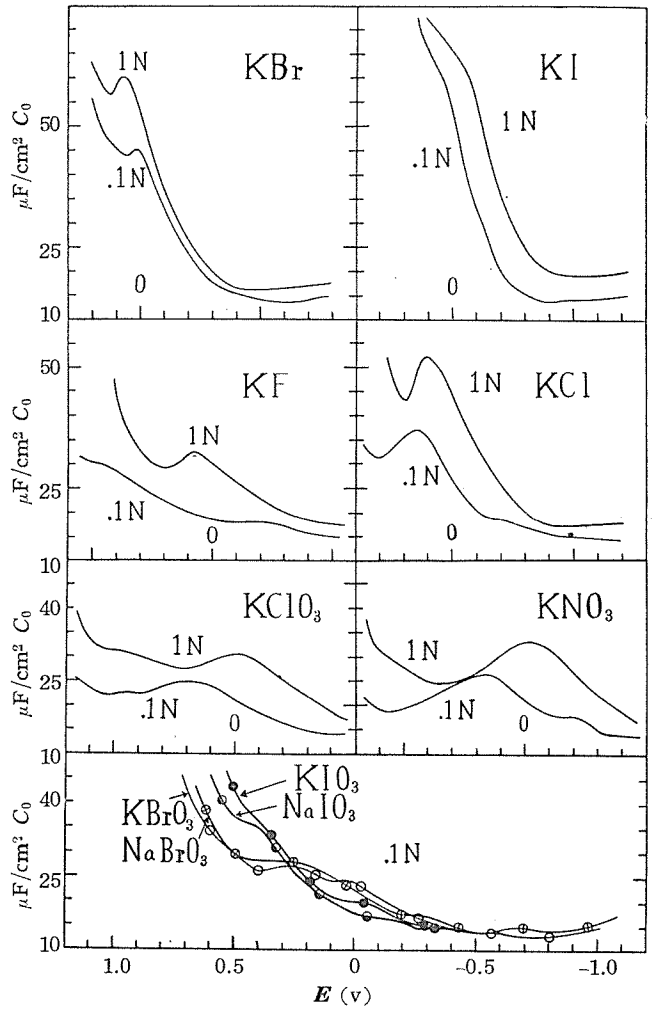

Fig. 4.

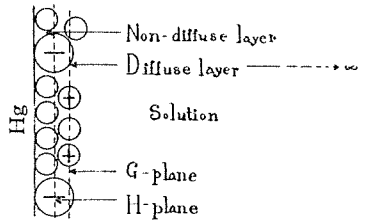

Fig. 5. Double layer model. Small circles without any sign stand for water molecules.

capacity between M- and H-plane K_{M-H} with dielectric constant ϵ_{M-H}, that between H- and G-plane K_{H-G} with ϵ_{H-G}, and the differential capacity of the Gouy layer C_G with ϵ_G, respectively.*

* Devanathan did not discriminate between ϵ_{M-H} and ϵ_{H-G}.

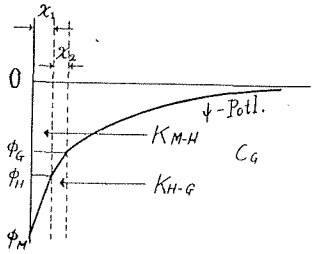

Fig. 6. Potential course in the double layer.

According to Devanathan, the total differential capacity of this double layer system is given by

$$\frac{1}{C}=\frac{1}{K_{M-H}}+\left(\frac{1}{K_{H-G}}+\frac{1}{C_G}\right)\left(1-\frac{dq_G}{dq}\right), \tag{8}$$

where q and q_G are the charge densities on the mercury surface and of the diffuse double layer, respectively. The integral and differential capacities are given by the electrostatics and the theory of Gouy, as

$$K_{M-H}=\varepsilon_{M-H}/4\pi x_1, \tag{9}$$

$$K_{H-G}=\varepsilon_{H-G}/[4\pi(x_2-x_1)], \tag{10}$$

and

$$1/C_G=d\phi_G/dq_G=\left(\frac{kT}{zeA}\right)\Big/\left(1+\frac{q_G}{4A^2}\right)^{\frac{1}{2}}, \tag{11}$$

where

$$A^2=\epsilon_G kTn/2\pi,$$

and in the case of 1-1 salts,

$$C_G=19.46\ (137.8\,c+q_G^2)^{\frac{1}{2}}. \tag{11'}$$

It is evident from eq. (8) that the total capacity becomes less, as the concentration of solution becomes smaller, because the diffuse layer capacity thereby becomes smaller and no longer negligible. Although we cannot say with certainty that q_G is zero at electrocapillary maxium (we can only say $q=0$), we can presume in general that the zero point of q_G may lie near this point. At this point C_G must have minimum value, as is clear from eq. (11) or (11'), at constant concentration.

This tendency of lowering of the capacity is practically noticeable in the cases of nitrate, fluoride and halogenate solutions of 0.1 N concentration. (Fig. 4) In the cases of 1 N solutions it is masked by the non-diffuse part of the double layer, because C_G becomes too large to be effective on the total capacity, cf. eq. (8).

It is noticed by comparing the capacity behaviours at 1 N and 0.1 N solutions in Fig. 4, that the capacity humps are more prominent in the former cases, which suggests that these are due to the behaviours in the non-diffuse part of the double layers. The capacity in this part would be inversely proportional to the ionic radius, as is evident

Table 2. Humps of differential double layer capacities and anionic properties.
K-salts.

	C_h (μF/cm^2)		Ionic radius[6] r (Å)	Interatomic distance[6] r_{12} (Å)	Ionic shape[6]
	1 N	0.1 N			
I	75	65	2.16		Monatomic
Br	60.5	45	1.95		
Cl	52	37	1.81		
F	32	30	1.36		
IO_3		33.5		1.83	Pyramidal
BrO_3		27		1.67	
ClO_3	30	22.5		1.48	
NO_3	33.5	26.5		1.22	Planar
$\frac{1}{2}SO_4$	48			1.51	Tetrahedral

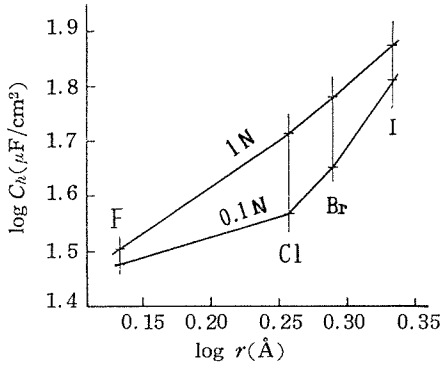

Fig. 7.

from eq. (9), if the dielectric constants were the same in all solutions. However, this is not the case in our results, as is shown in Table 2. Contrary to our presumption, the larger the ionic radius, the larger is the value of C_h. Fig. 7 shows how C_h depends upon r in the case of halogens, all of which have the same ionic shapes. Plots of log C_h at 1 N solutions give a straight line with a slope of 1.7. This slope is, of course, ascribed to the different polarizabilities of the anions, which are nearly proportional to ionic volumes.

We need not mention that the non-linearity in the case of 0.1 N solutions is the more prominent influence of diffuse double layer capacity C_G in the more dilute solutions.

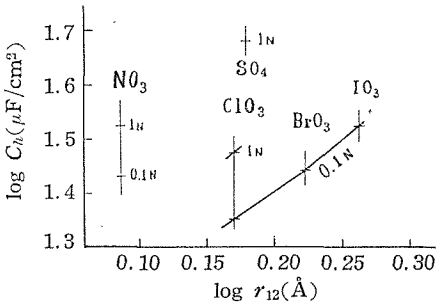

Fig. 8.

Halogenates seem to have the same tendency with almost the same slope, as is shown in Fig. 8, where log C_h is plotted against log r_{12}, i.e. logarithm of interatomic distance of each ion. Although we shall presumably obtain linearity at 1 N solutions, we cannot perform the experiment because of the limited solubilities of these salts.

In the same figure are plotted also log C_h values of other ions. It is not unexpected that they do not come on the halogenate line, because sulfate is a 2-valent ion and nitrate a plane triangular shaped ion, both of which are supposed to enhance the inner layer capacity values.

In view of the fact that this capacity hump is chiefly ascribed to the polarizability of the anionic species present at H-plane, we can assume that the phenomenon of hump is connected with the dielectric saturation of the adsorbed anions. That is, as the electrical field in the double layer is generally very large, the polarizabilities of the adsorbed anions in the region apart from zero potential have saturated values. However, in zero region, as the field strength becomes less, the polarizabilities tend to have more or less their normal values and the capacity values become larger. In other words, the capacity hump indicates the minimum of dielectric saturation at this potential. As this conclusion is intimately connected with the absolute potential, this is but a bold hypothesis, which must be examined from another evidence other than thermodynamic means.

The authors express their gratitude to Prof. I. Tachi for his continued interest and encouragement.

REFERENCES

(1) A. Watanabe, F. Tsuji and S. Ueda, This Bulletin, **33**, 91 (1955).
(2) A. Watanabe, F. Tsuji and S. Ueda, *ibid.*, **34**, 1 (1956).
(3) A. Watanabe, F. Tsuji, K. Nishizawa and S. Ueda, *ibid.*, **32**, 62 (1954).
(4) D. C. Grahame, *Chem. Rev.*, **41**, 441 (1947).
(5) M. A. V. Devanathan, *Trans. Faraday Soc.*, **50**, 373 (1954).
(6) L. Pauling, "Nature of Chemical Bond", Cornell Univ. Press, (1939).